Physical changes recorded by a deep diving seal on the Patagonian slope drive large ecological changes

N. AUBONE[1,2,3,*], M. SARACENO[1,2,3], M.L. TORRES ALBERTO[4,5], J. CAMPAGNA[6], L. LE STER[7,8], B. PICARD[7], M. HINDELL[9,10], C. CAMPAGNA[11], C.R. GUINET[7]

1 Centro de Investigaciones del Mar y la Atmósfera (CIMA/CONICET-UBA), Ciudad de Buenos Aires, Argentina
2 Departamento de la Atmósfera y los Océanos, FCEyN, Universidad de Buenos Aires, Ciudad de Buenos Aires, Argentina
3 Instituto Franco-Argentino para el Estudio del Clima y sus Impactos (UMI IFAECI/CNRS-CONICET-UBA), Ciudad de Buenos Aires, Argentina
4 Instituto de Investigaciones Marinas y Costeras (IIMyC/UNMdP-CONICET), Mar del Plata, Argentina
5 Instituto Nacional de Investigaciones y Desarrollo Pesquero (INIDEP), Mar del Plata, Argentina
6 Centro para el Estudio de Sistemas Marinos (CESIMAR/CENPAT-CONICET), Puerto Madryn, Argentina
7 Centre d'Etudes Biologiques de Chizé, UMR 7372, CNRS-La Rochelle Université, 79360 Villiers en Bois, France
8 Laboratoire d'Océanographie de Villefranche-sur-Mer, (UMR-CNRS 7093), Quai de la Darse, B.P. 8, 06238 Villefranche-sur-Mer
9 Institute for Marine and Antarctic Studies, University of Tasmania, Hobart, Tasmania, Australia
10 Antarctic Climate and Ecosystems CRC, University of Tasmania, Hobart, Australia
11 Wildlife Conservation Society, Marine and Argentina Programs, Buenos Aires, Argentina

* corresponding author, <nicolas.aubone@cima.fcen.uba.ar>

Abstract

The Patagonian slope is the region where Subantarctic waters and bathymetry give raise to physical and ecological processes that support a rich biodiversity and a large-scale industrial fisheries. Unique among the species that depend on this region is the deep diving southern elephant seal, *Mirounga leonina*. We report here on changes in the foraging behavior of a female seal explained by the combined effect of a cold and high salinity water mass and a decrease in surface chlorophyll-a concentration. Behavioral and oceanographic data from about 5,000 profiles of temperature, conductivity, pressure, light and prey encounters were collected within an area ranging 59.5-61°W and 46-47.5°S, at depths of 300-700 m, on the Patagonian slope, during November-December 2018. A decrease in temperature (0.15°C) and an increase in salinity (0.03) was found below the mixed layer, during December. Light data revealed a significant increase of irradiance in December (almost reaching the ocean bottom) associated with a decrease of chlorophyll-a in the upper levels. Concomitantly, the seal had a different diving behavior in December, foraging near the surface at

night and close to the bottom during daylight hours. Also, the seal doubled the prey capture attempts in December compared to November. This study revels the importance of ocean physical properties on seal's diving and foraging behavior, and how this changes, although small, can impact on seals diet and body composition during their post-breeding trips.

Keywords : Southwestern Atlantic Ocean, Patagonian Shelf Slope, Elephant Seals, *Mirounga leonina*, Malvinas Current.

Acknowledgments

This work was funded through a collaboration of the National Observation Service Mammal as Ocean observer (SNO-MEMO), CNES-TOSCA and WCS. This work was supported by European Organization for the Exploitation of Meteorological Satellites (EUMETSAT)/Centre National de la Recherche Spatial (CNES) through project DSP/OT/07-2118 and by Agencia Nacional de Promoción Científica y Tecnológica (Argentina), project PICT 2018-02433.

1. Introduction

The Argentine Continental Shelf is located in the Southwestern Atlantic (Figure 1). The shelf is broad and relatively shallow, with almost 850 km in its wider zone, a surface area of about 1.2 million km^2, an extension of 2400 km from north to south, and a smooth slope with a variable maximum depth ranging between 70 and 200 m [Parker et al., 1996; Violante and Cavallotto, 2011; Violante et al., 2014]. East of the 200 m isobath, the shelf-break is characterized by a steep slope that goes from 200 to 4000 m depth. In the upper portion of the slope, biological activity is enhanced due to large chlorophyll-a (chl-a) blooms during the austral spring and summer [Saraceno et al., 2005; Romero et al., 2006; Garcia et al., 2008, 2011]. The Malvinas Current (MC), which detaches from the Antarctic Circumpolar Current's northern front, flows northward along the shelf-break. The MC carries cold and rich nutrient waters that may play a role in the large chl-a concentrations through interaction with topography and consequent upwelling [Matano and Palma, 2008]. The collision of the MC with the Brazil Curren at ~38°S, makes the confluence region one of

65 the most energetic of the world, with eddies and meanders reaching 50°S eastward of the slope
66 [Piola et al., 1987; Chelton et al., 1990; Saraceno et al., 2009]. Thus, the shelf-break front and the
67 upper slope encompass a complex region that concentrates a diversity of top predators and other
68 species, some exploited by industrial fisheries [Martinetto et al., 2020; Rey and Huettmann, 2020].
69 The Southern elephant seal, *Mirounga leonina,* that breed and molt along the coast of the Península
70 Valdés represent one of the main top predators inhabiting these waters. These continuous and deep-
71 diving seals spend several months at sea foraging, coming back to the location from where they left
72 to breed or moult [Lewis et al., 2004]. After leaving the shore, post-breeding females cross the
73 continental shelf in 3-7 days. They forage for approximately two months in deep waters off the
74 shelf, while adult males usually forage along the outer part of the shelf break [Campagna et al.,
75 1998, 1999]. Post-breeding females on deep waters show a dive rate of 2.2 dives/hr and a mean dive
76 duration of 22.8 minutes, where the mean dive depth range from the ocean surface to the bottom of
77 the continental shelf (~80 m) and beyond the shelf-break (~ 600 m) [Campagna et al., 1998]. This
78 continuous and deep diving behavior lead to the idea of using seals as ocean samplers of physical,
79 biogeochemical and biological parameters by deploying on them small electronic devices
80 (biologgers) allowing the conduction of a broad range of studies linking seals foraging behavior to
81 the oceanographic environment [MEOP project; Boehlert et al., 2001; Guinet et al., 2014; Della
82 Penna et al., 2015].
83
84 Taking advantage of the high frequency temperature, salinity, light, pressure and accelerometry
85 measurements obtained with the instruments carried by one seal, we investigated how ocean bio-
86 physical features changed and how its foraging behavior and success responded to those
87 environmental changes. This paper also aimed at investigating the consistency between satellite
88 measurements (temperature and chl-a) as well as CMEMS (Copernicus Marine Environment
89 Monitoring Service) model outputs with the in-situ hydrographic profiles provided by one seal.
90

2. Data and Methods

2.1 In situ data

As part of an international collaboration between the Centre National de la Recherche Scientifique (CNRS), the Wildlife Conservation Society (WCS), the University of Tasmania (UTAS) and the University of Buenos Aires (UBA), nine adult female seals were tracked along the Patagonian shelf and outer ocean during the austral spring 2018. Following deployment procedures described in Campagna et al. [1998, 1999, 2006], seals were equipped with positional Argos and/or GPS systems, as well as different high frequency sampling sensors that record depth (pressure), temperature, conductivity, fluorescence, irradiance (light), and acceleration (Table 1). In oceanic Case 1 waters (i.e. waters whose optical properties are determined primarily phytoplankton concentration and dissolved organic matter), light attenuation (i.e. the variation of the irradiance signal with depth) quantifies the amount of light arriving at the ocean surface and is independent to solar angle and cloud cover, thus, it can be used as a proxy of phytoplankton concentration [Bricaud et al., 1998; Mobley et al., 2004; Jaud et al., 2012; Bayle et al., 2015]. The higher the phytoplankton concentration the greater is light attenuation from the surface within the water column (Jaud et al., 2012). Acceleration measurements associated with head movements provide an index of prey capture attempts (PCA) (see Goulet et al., 2019). Satellite tags and data loggers were deployed in October 2018, Península Valdés, Argentina, on breeding seal females prior to their departure to the sea for their post-breeding foraging trip. At the end of their foraging trip, females return to shore. After being located thanks to the satellite tag, they were recaptured to recover the loggers. For this study we focus in only one seal (ID 14903) that, after leaving Península Valdés on October 25, 2018, spent two months foraging in a relatively small region over the slope, near the 600 m isobath, and returned to the same departure location on January 10, 2019 (Figure 1). The studied seal was equipped with a CTD-SRDLT tag [Boehme et al., 2009], including Argos transmitter (PPT), light and accelerometry (12.5 Hz) sensors (Table 1). After recovering, the tag was calibrated following

the methodology from MEOP described in Roquet et al., [2001] and Siegelman et al., [2019]. The accuracy of each profile location is of the order of 2 km [Boehme et al., 2009].

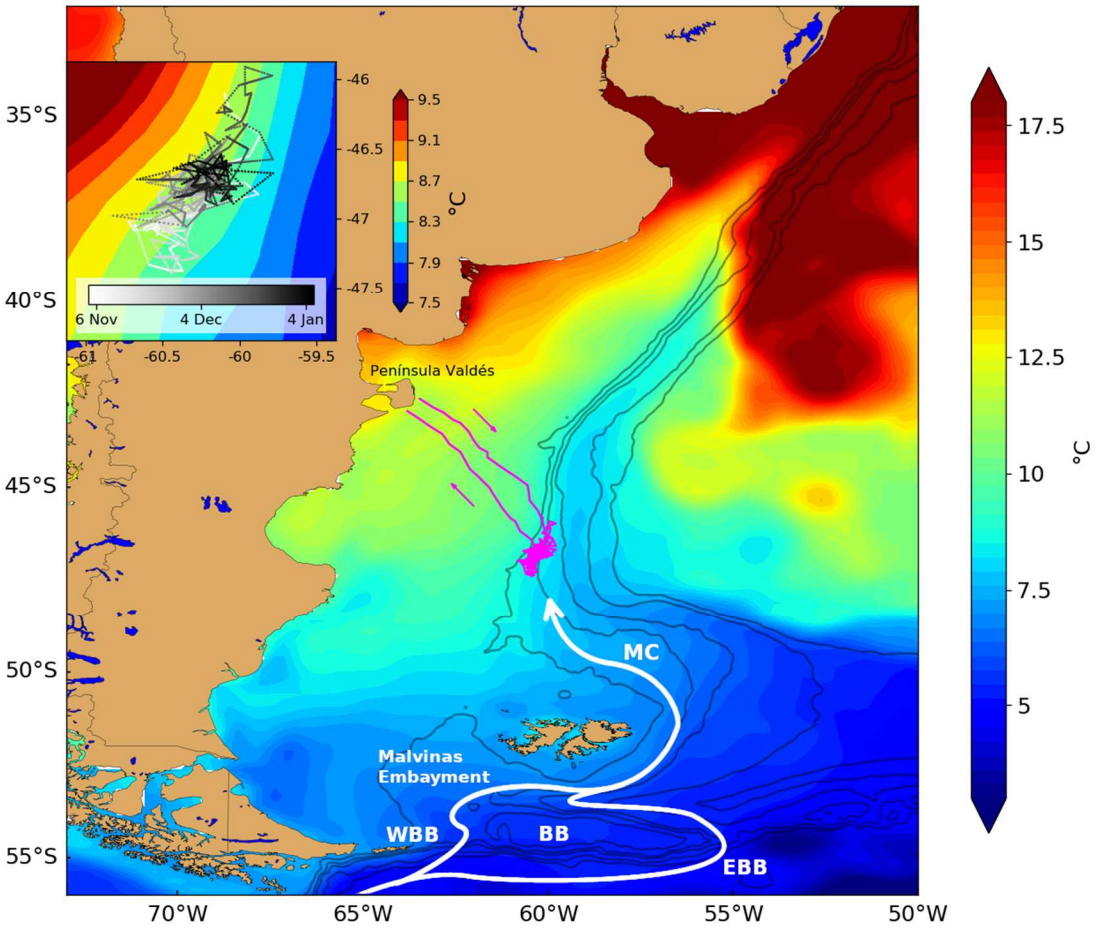

Figure 1. Tracks for the 73-day trip of one seal (magenta line) overlapping monthly-mean sea surface temperature (°C) for November 2018 from OSTIA (see section 2.3). Magenta arrows indicate direction of trajectory. The 200, 600, 1000, 2000 and 3000 m isobaths are indicated with thin black lines. The white arrow illustrates the main path of the upper slope portion of Malvinas Current (MC) through the western (WBB) and eastern (EBB) passages of the Burdwood Bank (BB). The top left inset zooms into the trajectory on the slope. Note that the scale of the temperature contours is different.

147 Table 1. Main characteristics of the instruments deployed on the studied seal.

CTD-SRDL	Range	Accuracy	Resolution	Frequency
Temperature	-5 to 35 °C	± 0.005°C	0.001°C	2 Hz
Salinity	0 to 50	± 0.01	0.002	2 Hz
Pressure	0 to 2000 dBar	2 dBar ± 0.01% / K	0.05 dBar	2 Hz
Light	8.31_x10^{-7} to 3000 µmol/m^2s	1%	0.1%	2 Hz

148

149

150 For the purpose of this study, and based on the sensor's accuracy, only dives deeper than 15 meters
151 were considered. Bottom depth, light and the temperature profiles associated with each dive were
152 extracted following the methodology described in Dragon et al., [2012a]. Each dive was divided
153 into a descent, bottom and ascent phase. The bottom phase corresponds to the period between the
154 end of the descent and the beginning of the ascent. The different dive phases were defined
155 according to Dragon et al., [2012a] using a custom-written MATLAB code (version 7.0.1; available
156 on request). Accelerometer data was processed following Viviant et al., [2010] and Gallon et al.,
157 [2013] using custom-written MATLAB code (available on request) to assess PCA. While PCA
158 provide fine scale insights of local variations of prey encounters, seal net foraging gain can be
159 assessed by monitoring change in seal body density (i.e. the change in the relative proportion in
160 between lipid and protein content) through its foraging trip. This is achieved by monitoring of the
161 descent rate, when the seal is sinking passively through the water column during special
162 resting/food processing dives qualified as 'drift dives' [Crocker et al., 1997; Biuw et al., 2003]. The
163 descent speed during these drift phases is directly related to buoyancy, with more buoyant seals (i.e.
164 with a higher lipid proportion) sinking at a slower rate compared with leaner ones [Crocker et al.,
165 1997; Biuw et al., 2003; Miller et al., 2012]. However, such 'drift rate' data obtained from time-
166 depth recorder tags can only provide a general temporal trend in body composition change and with
167 a temporal lag of about 3 to 6 days compared to change of PCA rate [Dragon et al., 2012b; Richard

et al., 2014, 2016]. Each dive was attributed to either day or night periods. This was defined according to the solar angle, taking into account the geographical location of the seal provided by the Argos transmitter and the time at the beginning of the dive (see Guinet et al., 2014).

The animal spent most of the time in a boundary region with strong year-round zonal temperature gradients (Figure 1, inset-panel), generated by the cold MC waters and the warmer continental shelf waters [Saraceno et al., 2004; Piola et al., 2013]. Over the two-month period, the seal tended to dive mostly in the southwestern part of the foraging area in November and in the northeastern part in December (Figure 1, inset-panel). Thus, to be able to compare the monthly mean temperature and salinity between November and December, the zonal movement of the seal was taken into account. To achieve this, we kept only with a sub-sample of the data (~28% of the total dives in the upper slope, i.e. 1146 from 4150 total profiles) after dividing the area in equal longitudinal bins and selecting the same amount of profiles on each longitude bin for November and December, discarding the rest. The selection of the discarded profiles was done randomly. This methodology was repeated a hundred times, to compute finally a mean temperature averaged from the hundred samples.

2.2 Numerical model and reanalysis data

The Operational Mercator global ocean analysis and forecast system (PSY4QV3R1) is based on NEMO ocean model [Madec et al., 2019] and provides 3D global ocean forecasts updated daily, starting in January 2016 for daily outputs and January 2007 for monthly outputs. It has a 1/12° degree horizontal resolution with regular longitude/latitude equi-rectangular projection, resolved over 50 vertical levels, ranging from 0 to 5500 m. Model outputs include daily and monthly mean files of temperature, salinity, currents, sea level and mixed layer depth among others. Comparison with satellite and Argo float data showed that the system correctly reproduced the general circulation and the complex hydrographic features of the Southwestern Atlantic Ocean (Artana et

al., 2018b). Model data is available through Copernicus Marine Environment Monitoring Service (CMEMS, http://marine.copernicus.eu/). To compare seal data with model, we downloaded daily values of temperature and salinity for the levels corresponding to the 0-600 m depth range in seal's foraging domain (46.2-47.3°S and 60.7-59.8°W). Valid seal measurements (after sensors stabilize in the water column) begin at ~18 m depth, thus, model values from 18 m were interpolated to seal location. Finally, a 4-hour moving average was applied to both series. For the temperature-salinity diagram (Figure 4), seal profiles were selected when the distance between a given profile and the nearest model grid point was less than 1 km. This procedure provided a total of 205 profiles for each data set. Also, to have the same number of vertical values per profile, we selected the values from the seal records that coincide with a depth level of the model (i.e. 32 levels, from the surface to 550 m).

Cloud cover mentioned in Section 3.2 is a product of ERA5 global reanalysis. We used monthly values of cloud area fraction in seal's foraging region, with a spatial resolution of 0.25°. Data is available at https://cds.climate.copernicus.eu/cdsapp#!/home

2.3 Satellite data

Sea surface temperature (SST) considered here was produced by the Group for High Resolution Sea Surface Temperature (GHRSST) and is provided by the Operational Sea Surface Temperature and Ice Analysis (OSTIA). The product merges in situ data, infra-red and micro-wave radiometers and has a 0.05° x 0.05° horizontal resolution [Bell et al., 2000; Stark et al., 2007; Donlon et al., 2012]. Near real time L4 product was downloaded from http://marine.copernicus.eu/. To compare SST with seal temperature measurements at 18 m (Figure 3a), data was interpolated to seal location and finally a 4-hour moving average applied.

Monthly mean composites and daily gridded L3 chlorophyll-a concentration MODIS-Aqua ocean color data, with a spatial resolution of 4 km from the Ocean Biology Processing Group (NASA/GSFC/OBPG) were downloaded from https://oceandata.sci.gsfc.nasa.gov.

3. Results

Sixty-three days out of the 73 day-long foraging trip were spent on the slope of the Patagonian shelf break (Figure 1). The seal covered 4,500 kilometers and performed a total of 4,951 dives (i.e. hydrographic profiles), from which 92% of them occurred over the slope. In this study we focus only on the data provided by the seal while foraging over the Patagonian slope from 4 of November 2018 to 6 of January 2019.

3.1 Physical environmental changes

Temperature and salinity profiles evidenced contrasted oceanographic changes over the study period between a warming upper layer (0-35 m) and cooling waters below (from 50 m to the bottom; Figure 2). In the upper layer, the depth-averaged temperature increased (1.6°C) within the two months due to higher net incoming heat radiation associated with the arrival of austral summer (Figure 2a). This change in temperature was accompanied by a salinity increase of 0.09 in the upper 35 m, enhanced in the last two weeks (Figure 2b). Waters below the upper layer show a very different behavior, with a mean temperature decrease in December of 0.25°C (Figure 2a) and an increase in salinity of 0.04 (Figure 2b). If we minimize the zonal displacement of the seal (see methods, Section 2.1), the temperature decrease and salinity increase in the subsurface layer accounts for 0.15°C and 0.03 respectively.

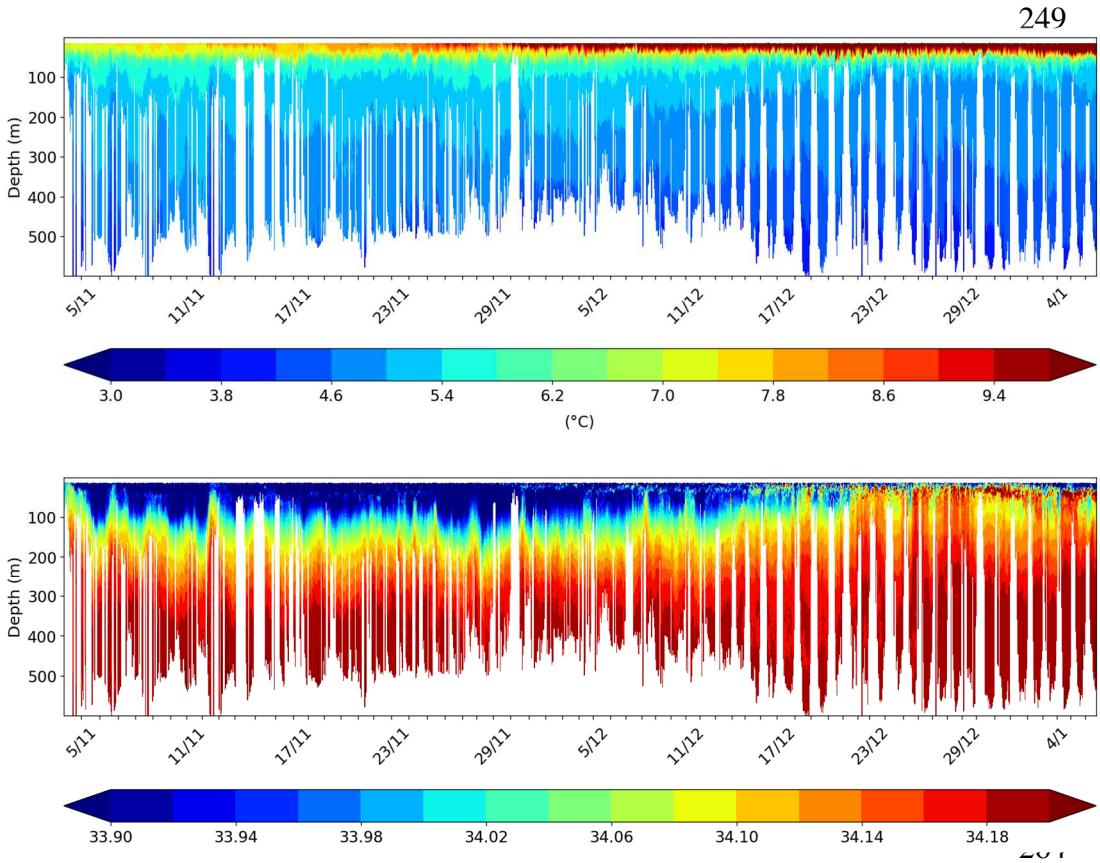

Figure 2. Temperature (°C, upper panel), and salinity (bottom panel) profiles measured by the seal in the Patagonian slope (top and bottom panels respectively).

Near surface temperature (T18) and salinity (S18) values obtained by the seal were compared with those from Mercator model and satellite observations following procedures described in Section 2 (Figure 3). The seal T18 signal presented visible discrepancies compared to Mercator temperature at 18 m and to OSTIA L4 surface values. Temperatures recorded by the seal were lower than OSTIA during both months, and slightly higher than Mercator in December. Also, there were amplitude differences between seal data and both series that result in a root mean square error of 0.62°C with OSTIA and 1°C with Mercator. Nevertheless, they all described the same temperature increase pattern during both months, and were highly correlated ($r = 0.91$ with Mercator and $r = 0.94$ with OSTIA, at the 99% significance level) (Figure 3, left panel). As we were unable to compare our data

277 with satellite surface salinity measurements with spatial and temporal resolution comparable to the
278 horizontal diving range of the seal, we only compared salinity recorded by the seal and Mercator
279 outputs at 18 m (Figure 3, right panel). Mercator salinity showed higher values in November and
280 early December compared to our data (root mean square error = 0.08), and a salinity decrease since
281 December 11, the opposite of what was observed in our records, that increased during all December.
282 Also, the two-month salinity time series were not significantly correlated; yet, if we split the series
283 by month we found a significant correlation in November (r = 0.5), and no correlation in
284 December.

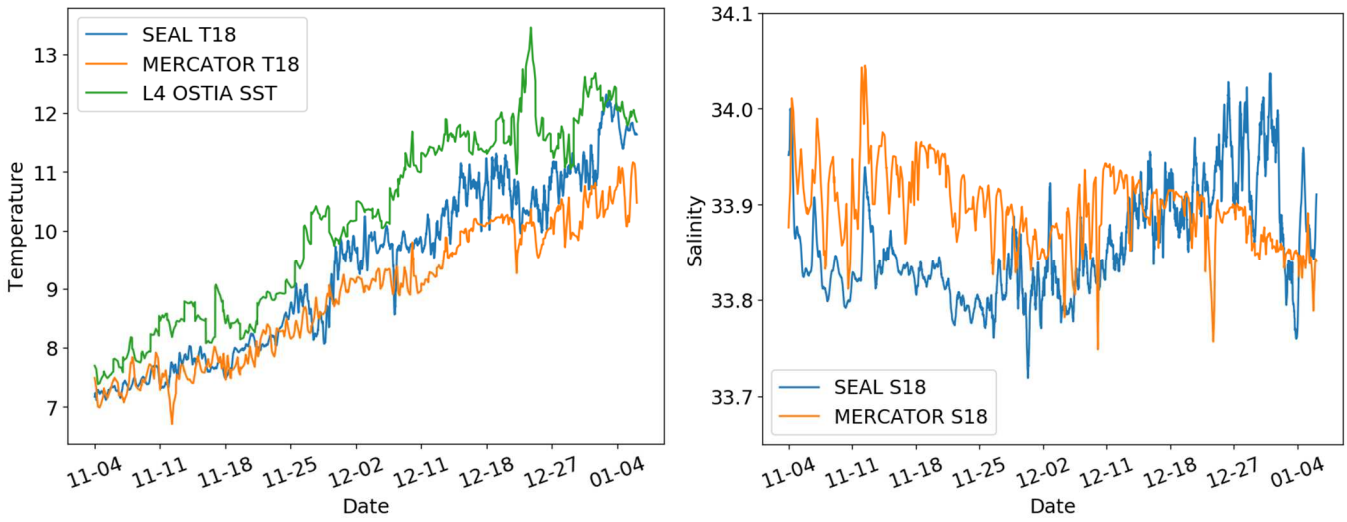

285

286 Figure 3. Four hours moving average of temperature at 18 m from seal records (blue) and Mercator (orange) and at surface for
287 OSTIA (green) (°C, left panel). Right panel shows the salinity from seal records at 18 m (blue), Mercator (orange).
288
289 Subsurface data obtained by the seal in the upper slope were compared with those from Mercator
290 model in a temperature-salinity diagram (Figure 4) following the methodology explained in Section
291 2.2. Following the water masses definitions described by Piola and Gordon [1989] and by
292 Maamaatuaiahutapu et al. [1994], the temperature and salinity distribution indicated that the
293 foraging region of the seal was composed mostly of three water masses: Subantarctic Surface
294 Waters (temperature > 5°C, salinity ~ 33.82), Subantarctic Mode Waters (temperature ~ 4.7°C,
295 salinity ~ 34.19) and Upper Antarctic Intermediate Waters (temperature < 4°C, salinity ~34.18)

(Figure 4a). A closer inspection of the bottom water distribution (blue box in Figure 4a) is coherent with the ~0.15°C December cooling observed in Figure 2, while a salinity change was imperceptible (Figure 4b). Some major differences arise when comparing seal data with Mercator temperature-salinity distribution. Subantarctic Surface Water for model distribution were less disperse in salinity but showed a strong dispersion in the transition through Subantarctic Mode Waters, that, in turn, presented a higher temperature, reaching 6°C (Figure 4c). The Antarctic Intermediate Waters for model data (blue box in Figure 4c) appeared as two distinct waters masses, one fresher and other saltier and slightly colder, the former being from November and the latter from December (Figure 4d). The cooling observed in December may be due to intrusions of the MC core [Piola et al., 2010; Matano et al., 2010; Combes and Matano, 2014] or to the increased transport of Upper Antarctic Intermediate Waters from the Eastern passage of the Burdwood Bank [Piola and Gordon, 1989; Matano et al., 2019].

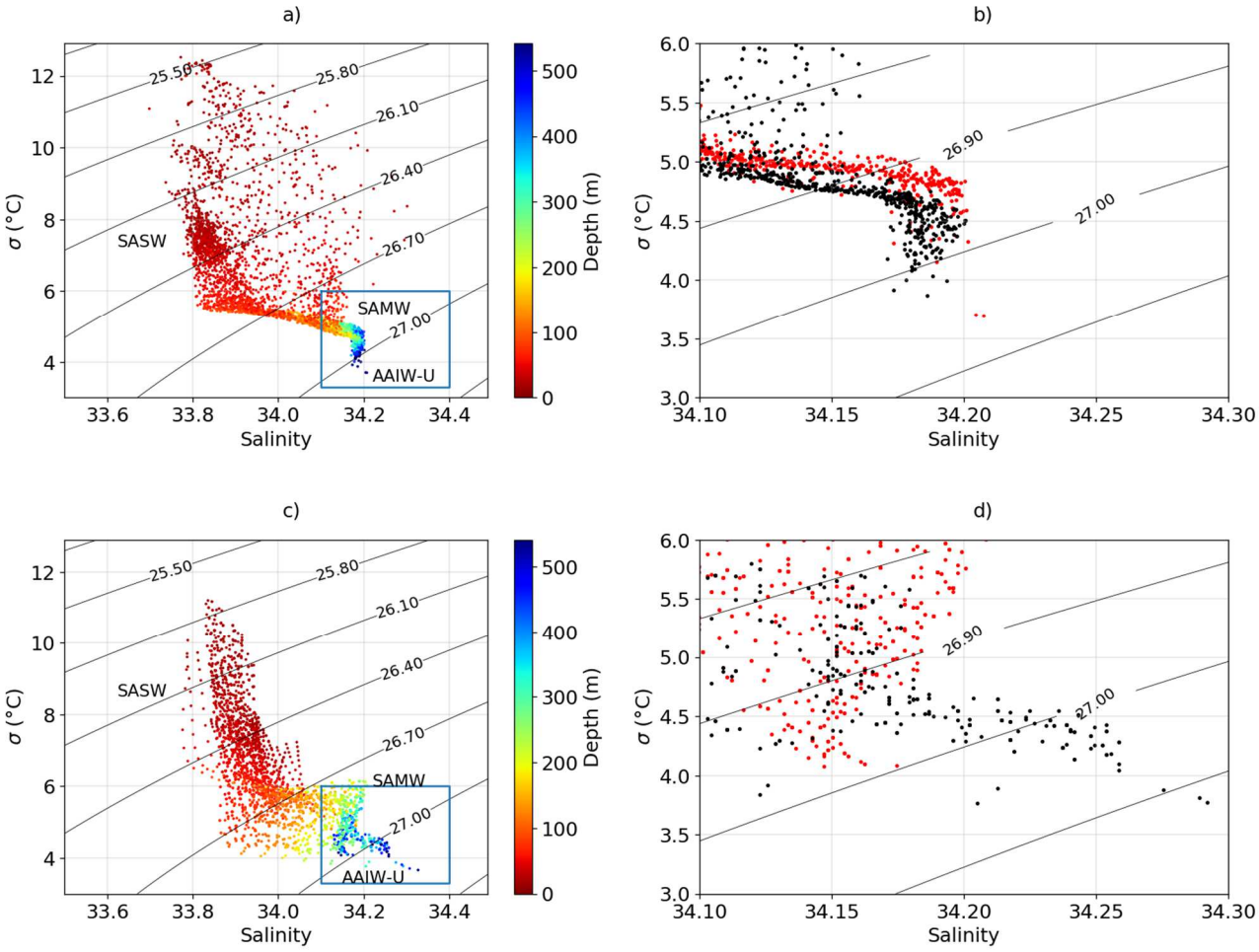

Figure 4. Potential temperature – salinity diagrams from data recorded by the seal (a) and Mercator outputs (c). The colorbar indicates the depth of each dot and the gray lines the potential density isolines (sigma-theta). Deep waters (indicated with a blue box on both diagrams) are amplified in panel b) for the data recorded by the seal and panel d) for Mercator. The red dots in panels b and d correspond to November data and the black ones to December. The different water masses are indicated in panels a,c as SASW (Subantarctic Surface Waters), SAMW (Subantarctic Mode Waters) and AAIW-U (Upper Antarctic Intermediate Waters).

3.2 Change in phytoplankton concentration

Light attenuation in open ocean waters partially depends on the concentration of inorganic and organic particles suspended within the water column. In particular, phytoplankton (quantified through active measurement of chlorophyll-a fluorescence) constitutes the main source of particles in suspension within the euphotic layer, and it has been shown to be the main cause of light attenuation for Case 1 waters [Bricaud et al., 1998; Jaud et al., 2012]. In November, the irradiance in the Patagonian upper slope region, where the seal spent time, reached more than -8 ln

(µmol/m²/s) only in the upper 150 m of the water column (Figure 5). However, the same amount of irradiance reached 500 m depth in December, revealing a sharp decline in phytoplankton concentration. Seasonal solar incidence angle and daylight duration also contributed, in a minor way, to light increase in December. Cloudiness also affects the amount of light that reaches the ocean surface. However, total cloud cover was higher in December compared to November (not shown). Thus, the irradiance increase observed between November and December can be mostly explained by the decrease in chlorophyll-a (chl-a hereafter) concentration.

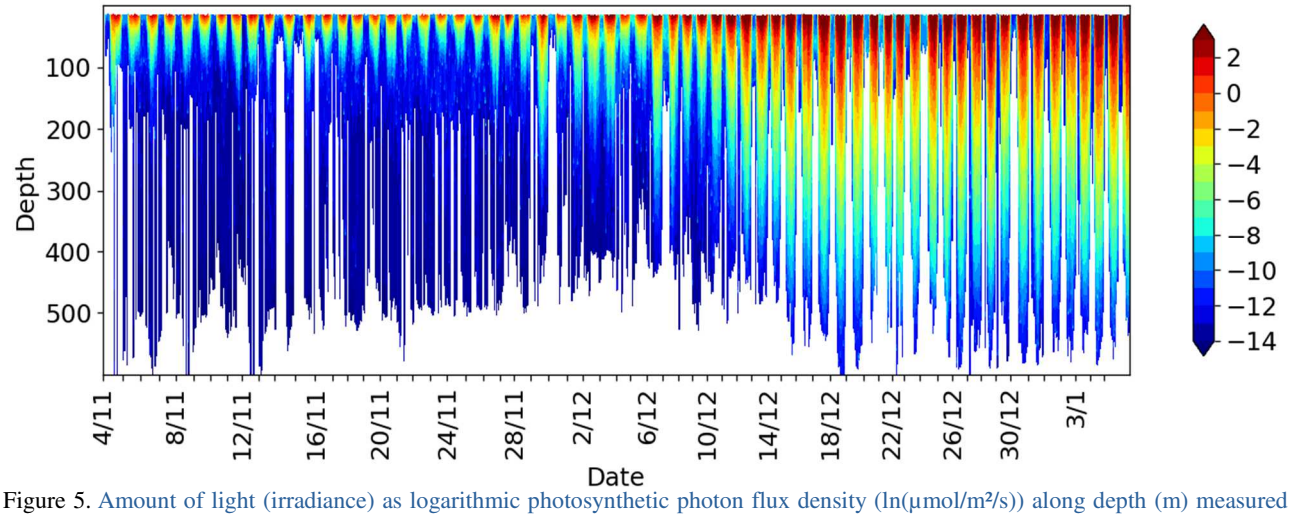

Figure 5. Amount of light (irradiance) as logarithmic photosynthetic photon flux density (ln(µmol/m²/s)) along depth (m) measured by the seal in the slope region during November and December.

In-situ assessments of phytoplankton concentration were consistent with the MODIS-Aqua ocean color satellite measurements over the study period for November 2018 (Figure 6a). This result revealed large amounts of chl-a (> 6 mg/m^3) over the region where the seal dove, and over the 200 m isobath, the shelf-break front (SBF). These large concentrations of chl-a generated a barrier of suspended particles that inhibited light beyond the upper layers. In December 2018 (Figure 6b), the chl-a concentration decreases (< 2 mg/m^3), thus allowing the light to reach greater depths. The chl-a concentration decrease was also observed in daily MODIS-Aqua ocean color chl-a and surface chl-a concentration estimated by seal irradiance data and a linear functional model (LFM) (Figure 6c).

The linear functional model described in Bayle et al. 2015 is a predictive tool enabling to infer chl-a concentration from irradiance along the water column through a per-profile functional approach based on a learning dataset of concomitant vertical profiles. Light in the ocean has a direct correlation with the vertical distribution of many marine organisms, ranging from zooplankton [Liu et al., 2003] to fish [Batty et al., 1990] and marine mammals [Horning and Trillmich, 1999]. Elephant seals depend on suitable and abundant prey (fishes and squid) present at the fronts [Campagna et al., 2007; Eder et al., 2010]. The area frequented by the studied animal, is associated with the SBF. The SBF has high concentrations of chl-a and high primary production, which would attract organisms of different trophic levels [Martinetto et al., 2020]. Moreover, the SBF is an area of intense fishing activity [Portela et al., 2012; Alemany et al., 2014] (Figure 6a,b). The main commercial species, at different times of the year, are Patagonian grenadier (*Macruronus magellanicus*), shortfin squid (*Illex argentinus*) and Argentine hake (*Merluccius hubbsi*) [Portela et al., 2012; Alemany et al., 2014]. Figure 6a,b shows that the fishing effort (in hours, Global Fishing Watch, 2020) in the SBF was much larger in December 2018 (18031 hours) than in November 2018 (4841 hours), and that the international fishing fleet concentrated north of the seal foraging ground. Figure 6 also shows that the largest fishing activity along the shelf-break did not correspond to the period of time when the largest chl-a concentration was observed.

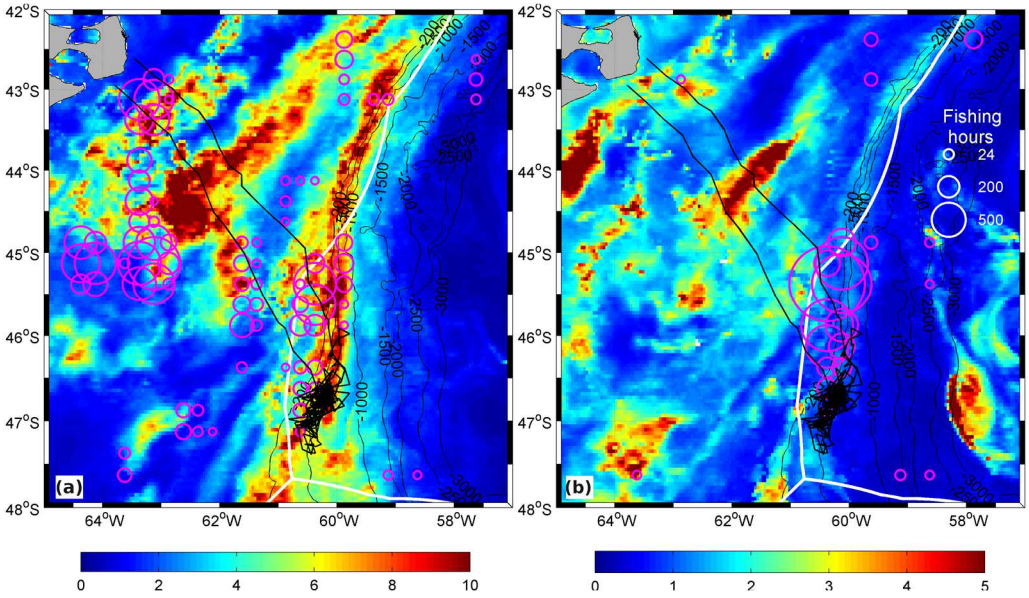

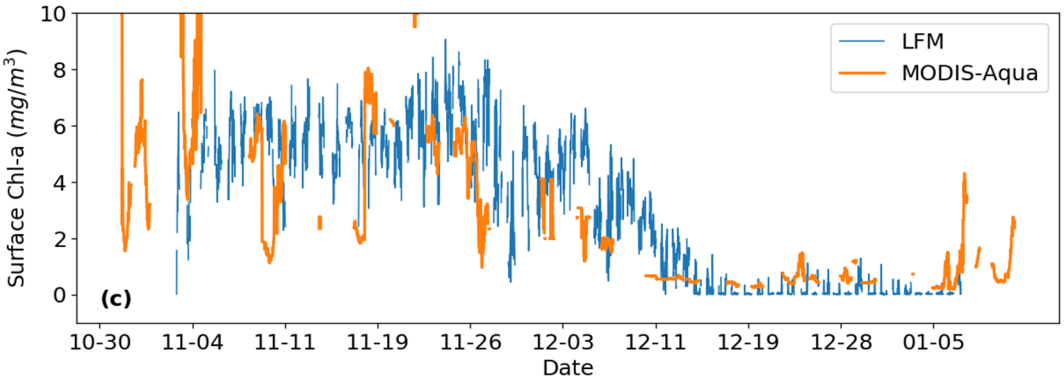

Figure 6. Modis-Aqua monthly mean chl-a concentration (mg/m^3) for November (a) and December (b) 2018. The magenta circles represent the fisheries activity for each month, the size is proportional to the fishing effort (hours). The white line represents the limit of the Argentine Exclusive Economic Zone. The black lines indicate the seal trajectory and the isobaths. Daily surface chl-a concentration (c) in mg/m^3 for satellite Modis-Aqua (orange) and estimated by the LFM method (blue).

3.3 Elephant seal foraging behavior

The overall mean diving depth of the seal was 263.8 ± 192.0 m at night, with a mean dive duration of 17.4 ± 4.3 minutes. During the day, the mean diving depth was 331.5 ± 186.7 m, with a mean dive duration of 19.8 ± 3.9 minutes.

To better understand how ocean dynamics and light can affect elephant sea foraging behavior we analyzed dive maximum depth (DMD) for each dive, and number of PCA performed. In November, DMD were either on shallow waters (<200 m) or sweeping the ocean bottom, avoiding the middle depths and with a minor difference between day and night (Figure 7). The sea floor (shading gray in figures 7 and 8) is an interpolation of GEBCO 2019 bathymetry (15 arc-second resolution) to seal diving locations, and DMD extending beyond the sea floor are due to possible errors on seal location or bathymetric chart product. In December, the animal dove predominantly (58%) near the surface at night (blue dots in Figure 7), and reached the ocean bottom (80%) during the day (red dots in Figure 7). The mean DMD increased from 337.5 ± 173.7 m in November to 359.4 ± 180.4 m in December and the mean dive duration increased from 17.6 ± 3.5 minutes in November (9.4 ± 3.3 minutes in the bottom phase) to 19.6 ± 4.5 minutes in December (11.1 ± 4.0 minutes in the bottom phase).

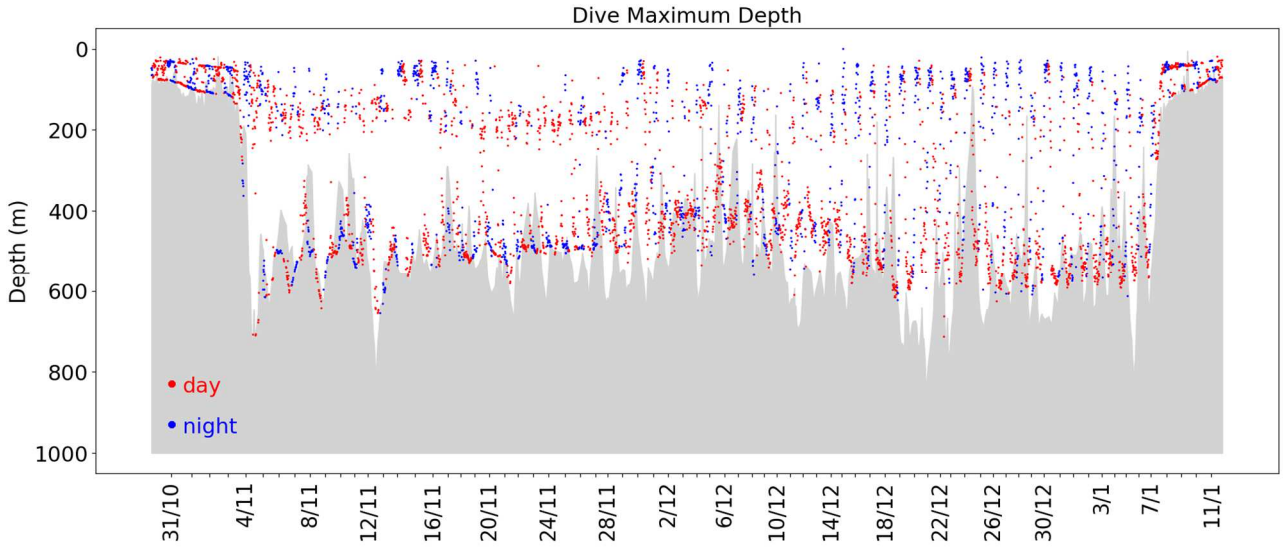

Figure 7. Dive maximum depth (DMD) with different colors for day (red) and night (blue). The shading gray is the bottom topography from GEBCO 2019 interpolated along the elephant seal diving trip.

Compared to November, December was characterized by a significant increase in number of PCA (287 versus 125 PCA per day) (Figure 8). Statistics for both DMD and PCA are summarized in Table 2. In agreement with early studies [Guinet et al., 2014; Gallon et al., 2013; Schreer et al., 2001], the majority of the PCA (~86%) occurred during the bottom phase of the dive. In November, 77% of the observed PCA were skimming the ocean bottom, both during day (red dots) and night (blue dots) and with the particularity that an increase of PCA near the surface can be seen between 13-17 of November (Figure 8). In December, the majority of the PCA occurs in the upper (< 300 m) part of the water column during night (54%) and in the lower part (> 300 m) during daylight hours (89%). A strong decrease of PCA, especially near the ocean bottom was observed between 21-23 of December.

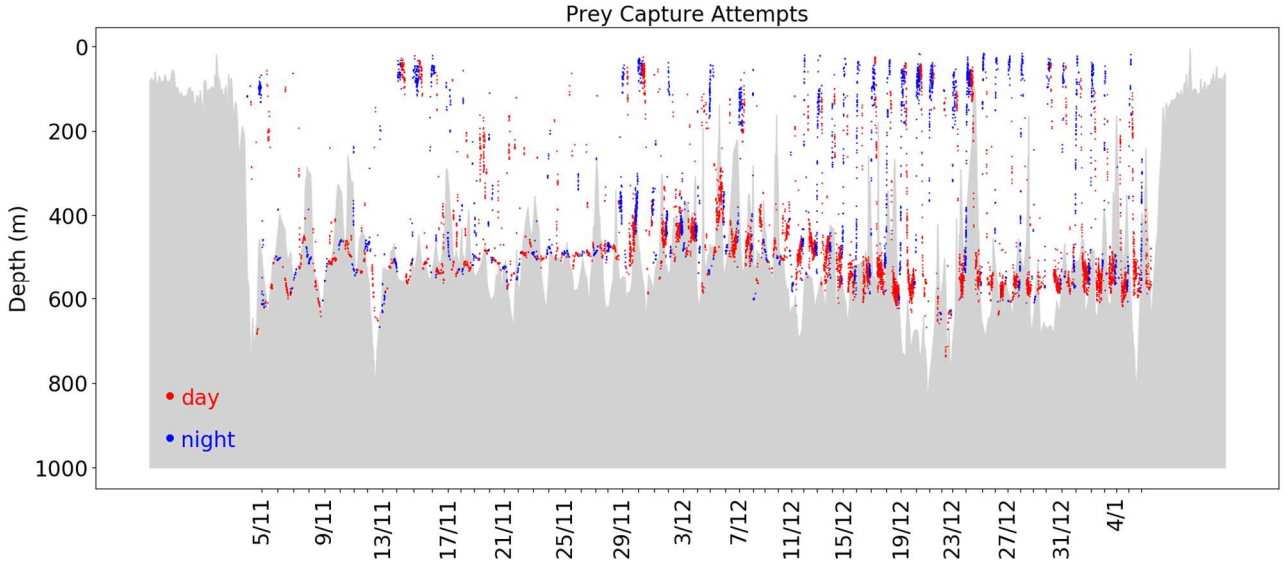

Figure 8. Depth location of prey capture attempts (PCA) with different colors for day (red) and night (blue). The shading gray is the bottom topography from GEBCO 2019 interpolated along the elephant seal diving trip.

Table 2. Total dives and percentages of DMD and PCA during November and December 2018. Upper water column (< 300 m) and lower water column (> 300 m).

	Dives		DMD		PCA	PCA	
	Total	Mean Duration (minutes)	Upper Water Column (%)	Lower Water Column (%)	Total	Upper Water Column (%)	Lower Water Column (%)
November	2093	17.6	40	60	3745	23	77
Day	1285	18.5	41	59	2194	20	80
Night	808	16.8	38	62	1551	29	71
December	2050	19.6	34	66	8617	24	76
Day	1287	21.2	20	80	5967	11	89
Night	763	18.0	58	42	2650	54	46

The monitoring of the female body density, reveals that seal density increased to remain high through the whole month of November and started to decrease (i.e. improvement of body condition due to an increase in lipid content, which is linked to a higher prey ingestion) by early December (Figure 9), which matches well with the change in environmental conditions (keeping in mind that there is a lag of 3 to 7 days between prey ingestion and body density changes [Dragon et al., 2012b; Richard et al., 2014, 2016]).

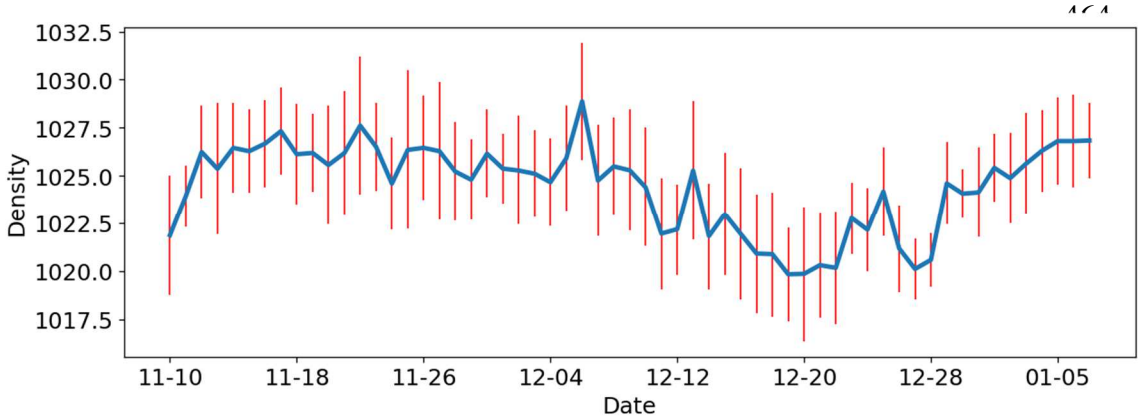

Figure 9. Seal daily mean density (kg/m^3) estimated along the trip (blue line) and standard deviations (red lines).

4. Summary and Discussion

High frequency data collected along the upper portion of the Patagonian slope during November and December 2018 by one post-breeding female elephant seal equipped with multiple sensors was used to investigate the interaction between ocean dynamics and seal diving and foraging behavior. Measurements obtained by the seal showed a decrease in temperature (0.15°C) and a salinity increase (0.03) below the mixed layer during December in the Patagonian slope, at 46-47.5°S. Temperature outputs from Mercator model at 18 m and OSTIA satellite data were in agreement with the increase pattern observed from seal data at 18 m. Nevertheless, our records showed higher temperatures than Mercator in December, and discrepancies in amplitude oscillations. On the other hand, salinity outputs from Mercator showed major differences with that obtained by the seal at 18 m, mostly in December, when Mercator data showed an opposite pattern. The differences between seal and Mercator data may be due to a mismatch between seal location and ARGOS positioning system, but also to the fact that seal's data used for the comparison was from around 18 meters

488 (where sensors stabilize and give more accurate measurements). Given that temperature and salinity
489 profiles recorded by the seal indicate a mixed layer depth of ~25 m in November and ~18 m in
490 December (not shown), measuring at this depth level may lead to uncertainties, mostly in
491 December. Also, SRLD-CTD sensors could surfer an erosion of its accuracy during the seal's trip,
492 specially for salinity measurements [Santini et al., 2018]. Light data also revealed a significant
493 increase of irradiance in December (almost reaching the ocean bottom) associated with a decrease
494 of chl-a in the upper levels revealed by our records and satellite Modis-Aqua data. Indeed, the
495 largest concentration of chl-a values in the Patagonian shelf and slope are usually observed in
496 November, during the austral spring bloom [Saraceno et al., 2005; Romero et al., 2006; Rivas et al.,
497 2006] and start decreasing in December due to nutrient consumption and ocean stratification that
498 inhibits the upwelling of nutrients to the euphotic zone.
499
500 Fishing effort in December (larger compared to November,) was concentrated north of the seal
501 foraging ground. The spatial mismatch between the fishing activity and the seal foraging ground
502 can be due to several causes, as seal trying to avoid fishing lines and nets and/or a different spatial
503 distribution or differences in the targeted fish/squids species by seal and fisheries. Indeed, the seal
504 might be eating preys that are not of commercial interest, like lantern fish (Myctophids) that are
505 very common in this area [Figueroa et al., 1998; Eder et al., 2010; McGovern et al., 2019]. Yet, we
506 do not have data to explain the spatial distribution mismatch. Also, the largest fishing activity along
507 the shelf-break did not corresponded to the period of time when the largest chl-a concentration was
508 observed. This fact can be explained considering different possibilities: (i) the most interesting
509 commercial species arrived in December with the colder and saltier water mass observed above; (ii)
510 the species that took advantage of the large phytoplankton bloom in November grow enough so in
511 December became prey of commercial species. Last but not least, the fact that both in November
512 and in December relatively large chl-a concentrations were observed along the upper portion of the

513 Patagonian slope in comparison to adjacent waters is a clear indication that a physical forcing
514 related to the bathymetry drives the large concentration of chl-a observed.
515
516 The elephant seal also showed a distinct behavior during the two-months trip. In December, the
517 PCA increased more than double with respect to November with the seal diving preferentially at
518 surface during the night and in the bottom layers during the day. The increase in PCA observed in
519 December can be attributed to a higher concentration of prey items due to the arrival of preys with
520 cold nutrient rich Antarctic Intermediate Waters. This result was also reflected in the larger fishing
521 effort detected in December. The density change of the seal along the trip, reflected quite well the
522 increment of PCA at the beginning of December. Moreover, the density increase observed around
523 the 23-26 of December matched with the observed decrease in PCA between 21-23 of December.
524 The increase of PCA in December can be seen both in the surface and bottom layers, suggesting that
525 the arrival preys migrated along the whole water column in response of light variability. Results
526 also showed that in December DMD increased 6% compared to November (66% of the dives in
527 December were below 300 m depth against 60% in November) and an increase of 2 minutes in
528 dives duration. These results are in agreement with previous studies that found a negative
529 correlation between surface chl-a concentration and both DMD and dive duration [Dragon et al.,
530 2010].
531
532 The relationship between prey location in the water column and light is known to dominate seals
533 diving behavior [Jaud et al., 2012; Guinet et al., 2014]. Several studies have shown that light level
534 precisely controls the vertical distribution of many species, in particular myctophids, which are part
535 of the seals diet [Catul et al., 2011]. Lower surface chl-a concentration means higher light
536 penetration, thus a deeper distribution of myctophids species. According to this, seal behavior in
537 December suggests that shallower dives during the night are related to preys that tend to concentrate
538 near the surface. During the day, as light increases in the water column, prey items tend to displace

539 to higher depths, and so does the seal, with predominant DMD and PCA near the seabed in
540 December.
541
542 We can expect that low irradiance (light) in November due to high chl-a concentration should be
543 associated with myctophids prey located in shallower waters, conditioning the seal to dive and
544 forage closer to the surface. However, November data showed that the seal dived predominantly
545 near the seabed, where most of the PCA were detected. This result suggests that a different prey
546 item, other than myctophids, can be the main diet for seals in the ocean bottom. This hypothesis is
547 in agreement with McIntyre et al., [2011] which came to the conclusion that seals can have different
548 forage strategies and dives, reaching greater depths at night compared with the day and that the
549 change can be associated with foraging of different prey resources. Furthermore, Goulet et al.,
550 [2020] suggest that female seals in Península Valdés are mainly pursuing larger or harder to catch
551 prey that do not produce bioluminescence as a predator defense and are probably more dispersed in
552 the water column.
553
554 The Patagonian slope is a very complex region, where subantarctic waters and bathymetry give
555 raise to a unique area of ecological processes and one of the greatest fisheries in the world. The
556 uniqueness of simultaneous high resolution in-situ data (physical, biogeochemical and biological)
557 collected by seals are a valuable resource to address oceanographic research and to calibrate and
558 validate ocean numerical models and satellite data. In particular, the data obtained from one seal
559 allowed us to improve our knowledge of the MC in the upper portion of the Patagonian slope, at
560 47°S, and also to link the sharp change in the water masses to the animal behavior. To deepen this
561 study, future campaigns in the region are thought to track fully equipped male elephant seals that
562 are known to dive preferentially in the Patagonian slope. Also, it is planned to incorporate
563 photographic cameras to the seals to try to unveil the prey items. Complementary data from
564 fisheries will also help elucidate the diving behavior and forage strategies in the region.

565
566 **References**

567
568 Alemany D., Acha E.M., and Iribarne O.O. (2014). Marine fronts are important fishing areas for
569 demersal species at the Argentine Sea (Southwest Atlantic Ocean). Journal of sea research, 87,
570 56-67

571
572 Artana C., Lellouche J.M., Sennéchael N., and Provost C. (2018a). The open-ocean side of the
573 Malvinas Current in Argo floats and 24 years of Mercator Ocean high-resolution (1/12) physical
574 reanalysis. Journal of Geophysical Research: Oceans, 123, 8489–8507.
575 https://doi.org/10.1029/2018JC014528

576
577 Artana, C., Lellouche, J.M., Park, Y.H., Garric, G., Koenig, Z., Sennéchael, N., et al. (2018b).
578 Fronts of the Malvinas Current System: Surface and Subsurface Expressions Revealed by
579 Satellite Altimetry, Argo Floats, and Mercator Operational Model Outputs. Journal of
580 Geophysical Research: Oceans, 123(8), 5261–5285. https://doi.org/10.1029/2018JC013887

581
582 Batty R., Blaxter J., Richard J. (1990). Light intensity and the feeding behaviour of herring, Clupea
583 harengus. Marine Biology 107: 383–388

584
585 Bayle S., Monestiez P., Guinet C., Nerini D. (2015). Moving toward finer scales in oceanography:
586 Predictive linear functional model of Chlorophyll *a* profile from light data. Prog. Oceanogr.
587 Volume 134, Pages 221-231, ISSN 0079-6611, doi : 10.1016/j.pocean.2015.02.001

588
589 Bell M. J., Forbes R.M. and Hines A. (2000). Assessment of the FOAM global data assimilation
590 system for real-time operational ocean forecasting. J. of Marine Systems, 25(2000) 1-22

591

592 Biuw, M., McConnell, B., Bradshaw, C.J.A., Burton, H. and Fedak, M. (2003). Blubber and
593 buoyancy: monitoring the body condition of free-ranging seals using simple dive characteristics.
594 J. Exp. Biol. 206, 3405–3423. (doi:10.1242/jeb.00583)

595

596 Blanke B., and Raynaud S. (1997). Kinematics of the Pacific Equatorial Undercurrent: a Eulerian
597 and Lagrangian approach from GCM results. J. Phys. Oceanogr., 27, 1038-1053

598

599 Boehlert G.W., Costa D.P., Crocker D.E., Green P., O'Brien T., Levitus S., Le Boeuf B.J. (2001).
600 Autonomous Pinniped Environmental Samplers: Using Instrumented Animals as Oceanographic
601 Data Collectors. J. Atmos. Oceanic Technol. 18 (11): 1882–1893

602

603 Boehme L., Lovell P., Biuw M., Roquet F., Nicholson J., Thorpe S.E., Meredith M.P. and Fedak M.
604 (2009). Technical note: Animal-borne CTD-satellite relay data loggers for real-time
605 oceanographic data collection. Ocean Sci., 5, 685–695

606

607 Bricaud A., Morel A., Babin M., Allali K., Claustre H. (1998) .Variations of light absorption by
608 suspended particles with chlorophyll a concentration in oceanic (case 1) waters: Analysis and
609 implications for bio-optical models. Journal of Geophysical Research 103: 31,033–031,044

610

611 Campagna C., Quintana F., Le Boeuf B.J., Blackwell S., Crocker D. (1998). Diving behaviour and
612 foraging ecology of female southern elephant seals from Patagonia. Aquatic Mammals 4, 1–11

613

614 Campagna C., Fedak M.A., McConnell B.J. (1999). Postbreeding distribution and diving behavior
615 of adult male southern elephant seals from Patagonia. Journal of Mammalogy 80, 1341–1352

Campagna, C., Piola, A.R., Rosa Marin, M., Lewis, M., & Fernández, T. (2006). Southern elephant seal trajectories, fronts and eddies in the Brazil/Malvinas Confluence. *Deep-Sea Research Part I: Oceanographic Research Papers*, *53*(12), 1907–1924. https://doi.org/10.1016/j.dsr.2006.08.015

Campagna C., Piola A.R., Marin M.R., Lewis M., Zajaczkovski U., and Fernández T. (2007). Deep divers in shallow seas: Southern elephant seals on the Patagonian shelf. Deep Sea Research Part I: Oceanographic Research Papers, 54(10), 1792-1814

Catul V.,Gauns M., Karuppasamy P. (2011). A review on mesopelagic fishes belonging to family Myctophidae. Reviews in Fish Biology and Fisheries 21: 339–354

Chelton D.B., Schlax M. G., Witter D.L. and Richman J.G. (1990). GEOSAT altimeter observations of the surface circulation of the Southern Ocean, J. Geophys. Res., 95, 17,877–17,903

Combes, V., and Matano, R.P. (2014). A two-way nested simulation of the oceanic circulation in the Southwestern Atlantic, J. Geophys. Res. Oceans, 119, 731–756, doi:10.1002/2013JC009498

Crocker, D., Le Boeuf B. and Costa, D. (1997). Drift diving in female northern elephant seals: Implications for food processing. Canadian Journal of Zoology. 75. 27-39. 10.1139/z97-004

Della Penna, A., De Monte, S., Kestenare, E. et al., (2015). Quasi-planktonic behavior of foraging top marine predators. Sci Rep 5, 18063. https://doi.org/10.1038/srep18063

640 Donlon C.J., Martin M., Stark J., Roberts-Jones J., Fiedler E. and Wimmer W. (2012). The
641 Operational Sea Surface Temperature and Sea Ice Analysis (OSTIA) system. Remote Sensing of
642 the Environment. doi: 10.1016/j.rse.2010.10.017 2011
643
644 Dragon A.C., Monestiez P., Bar-Hen A., Guinet C. (2010). Linking foraging behaviour to physical
645 oceanographic structures: Southern elephant seals and mesoscale eddies east of Kerguelen
646 Islands. Progress in Oceanography 87: 61–71
647
648 Dragon A.C., Bar-Hen A., Monestiez P., Guinet C. (2012a). Horizontal and vertical movements as
649 predictors of foraging success in a marine predator. Mar Ecol Prog Ser 447:243–257.
650 10.3354/meps09498
651
652 Dragon A.C., Bar-Hen A., Monestiez P., Guinet C. (2012b). Comparative analysis of methods for
653 inferring successful foraging areas from Argos and GPS tracking data. Mar Ecol Prog Ser
654 452:253-267. https://doi.org/10.3354/meps09618
655
656 Eder E.B., Lewis M.N., Campagna C. and Koch P.L. (2010). Evidence of demersal foraging from
657 stable isotope analysis of juvenile elephant seals from Patagonia. Marine Mammal Science, 26(2),
658 430-442
659
660 Figueroa D.E, Díaz de Astarloa J.M., Martos P. (1998). Mesopelagic fish distribution in the
661 southwest Atlantic in relation to water masses. Deep-Sea Res I Oceanogr Res Pap 45:317-332
662

Gallon S., Bailleul F., Charrassin J.B., Guinet C., Bost C.A., Handrich Y., et al. (2013). Identifying foraging events in deep diving southern elephant seals, Mirounga leonina, using acceleration data loggers. Deep Sea Res Part II Top Stud Oceanogr. 2013;88–89: 14–22

Garcia, V.T, Garcia, C.A.E., Mata, M.M., Pollery, R.C., Piola, A.R., Signorini, S.R., McClain, C.R., Iglesias-Rodríguez, M.D. (2008). Environmental factors controlling the phytoplankton blooms at the Patagonia shelf-break in spring. Deep-Sea Research Part II, 55, 1150-1166. doi:10.1016/j.dsr.2008.04.011

Garcia, C.A.E., Garcia, V.T, Dogliotti, A.I., Ferreira, A., Romero, S.I., Mannino, A., Souza, M.S., Mata, M.M. (2011). Environmental conditions and bio-optical signature of a coccolithophorid bloom in the Patagonian shelf. Journal of Geophysical Research, 116, C03025. doi:10.1029/2010JC006595

Global Fishing Watch. (2020). http://www.globalfishingwatch.org

Goulet, P., Guinet, C., Swift, R., Madsen, P.T., & Johnson, M. (2019). A miniature biomimetic sonar and movement tag to study the biotic environment and predator-prey interactions in aquatic animals. Deep Sea Research Part I: Oceanographic Research Papers,148, 1-11

Goulet, P., Guinet, C., Campagna, C., Campagna, J., Tyack, P.L., & Johnson, M. (2020). Flash and grab: deep-diving southern elephant seals trigger anti-predator flashes in bioluminescent prey. Journal of Experimental Biology, 223(10)

687 Guerrero, R.A., Baldoni, A.G., Benavides, H.R. (1999). Oceanographic conditions at the southern
688 end of the Argentine continental slope. INIDEP DOC. CIENT., 5, pp. 7-22
689
690 Guinet C., Vacquié-Garcia J., Picard B., Bessigneul G., et al. (2014). Southern elephant seal
691 foraging success in relation to temperature and light conditions: insight into prey distribution.
692 Mar Ecol Prog Ser 499:285-301. https://doi.org/10.3354/meps10660
693
694 Horning M., Trillmich F. (1999). Lunar cycles in diel prey migrations exert a stronger effect on the
695 diving of juveniles than adult Galapagos fur seals. Proceedings of the Royal Society of London
696 Series B: Biological Sciences 266:1127–1132
697
698 Jaud T., Dragon A.C., Garcia J.V., Guinet C. (2012). Relationship between Chlorophyll a
699 Concentration, Light Attenuation and Diving Depth of the Southern Elephant Seal Mirounga
700 leonina. PLoS ONE 7(10): e47444. doi:10.1371/journal.pone.0047444
701
702 Lewis, M., Campagna, C., & Zavatti, J. (2004). Annual cycle and inter-annual variation in the haul-
703 out pattern of an increasing southern elephant seal colony. Antarctic Science, 16, 219-226
704
705 Liu S.H., Sun S., Han B.P. (2003). Diel vertical migration of zooplankton following optimal food
706 intake under predation. Journal of plankton research 25: 1069–1077
707
708 Maamaatuaiahutapu, K., Garçon, V. C., Provost, C., Boulahdid, M. and Bianchi, A. A. (1994).
709 Spring and winter water mass composition in the Brazil-Malvinas Confluence, Journal of
710 Marine Research, 52, 397–426. https://doi.org/10.1357/0022240943077064
711

712 Madec G., Bourdallé-Badie R., Chanut J., Clementi E., Coward A., Ethé C., et al. (2019). NEMO
713 ocean engine (Version v4.0). Notes Du Pôle De Modélisation De L'institut Pierre-simon Laplace
714 (IPSL). Zenodo. http://doi.org/10.5281/zenodo.3878122
715
716 Martinetto, P., Alemany, D., Botto, F., Mastrángelo, M., Falabella, V., Acha, E.M., et al. (2020).
717 Linking the scientific knowledge on marine frontal systems with ecosystem services. *Ambio*,
718 *49*(2), 541–556. https://doi.org/10.1007/s13280-019-01222-w
719
720 Matano R.P., and Palma E.D. (2008). On the upwelling of downwelling currents. Journal of
721 Physical Oceanography, 38, 2482–2500. https://doi.org/10.1175/2008JPO3783.1
722
723 Matano, R.P., Palma, E.D., Piola, A.R. (2010). The influence of the Brazil and Malvinas Currents on
724 the southwestern Atlantic Shelf circulation. Ocean Science, 6(4), 983–995.
725 https://doi.org/10.5194/os-6-983-2010
726
727 Matano, R.P., Palma, E.D., & Combes, V. (2019). The Burdwood Bank circulation. Journal of
728 Geophysical Research: Oceans, 124. https://doi.org/10.1029/2019JC015001
729
730 McGovern, K.A., Rodríguez, D.H., Lewis, M.N., & Davis, R.W. (2019). Diving classification and
731 behavior of free-ranging female southern elephant seals based on three-dimensional movements
732 and video-recorded observations. Marine Ecology Progress Series, 620, 215-232
733
734 McIntyre T., Bornemann H., Plötz J., Tosh C.A., Bester M.N. (2011). Water column use and forage
735 strategies of female southern elephant seals from Marion Island. Mar Biol 158: 2125–2139
736

MEOP (Marine Mammals Exploring the Oceans Pole to Pole) project. www.meop.net

Miller, P.J.O., Biuw, M., Watanabe, Y.Y., Thompson, D. and Fedak, M.A. (2012). Sink fast and swim harder! Round-trip cost-of-transport for buoyant divers. J. Exp.Biol. 215, 3622-3630

Mobley, C.D., Stramski, D., Bissett, W.P., Boss, E., (2004). Optical modeling of ocean waters: Is the Case 1 –Case 2 classification still useful? Oceanography 17 (2), 60-67

Parker G., Violante R.A. and Paterlini C.M. (1996). Fisiografía de la Plataforma Continental. In : Ramos, V. & Turic, M. (eds) Geología y Recursos Naturales de la Plataforma Continental Argentina. Relatorio XIII Congreso Geológico Argentino. Asociación Geológica Argentina, Buenos Aires, 1–16

Piola A.R., Figueroa H.A., and Bianchi A.A. (1987). Some aspects of the surface circulation south of 20°S revealed by First GARP Global Experiment drifters, J. Geophys. Res., 92, 5101-5114

Piola A.R., Gordon A.L. (1989). Intermediate waters in the southwest South Atlantic. Deep Sea Research Part A. Oceanographic Research Papers, Volume 36, Issue 1, 1989, Pages 1-16, ISSN 0198-0149, https://doi.org/10.1016/0198-0149(89)90015-0

Piola, A.R., Martínez Avellaneda, N., Guerrero, R.A., Jardón, F.P., Palma, E.D., Romero, S.I. (2010). Malvinas-slope water intrusions on the northern Patagonia continental shelf, Ocean Sci., 6, 345–359

762 Piola A.R., Franco B.C., Palma E.D., Saraceno M. (2013). Multiple jets in the Malvinas Current. J.
763 Geophys. Res. Oceans, 118 (2013), pp. 2107-2117, 10.1002/jgrc.20170
764
765 Portela J., et al. (2012). Management Strategies to Limit the Impact of Bottom Trawling on VMEs
766 in the High Seas of the SW Atlantic, Marine Ecosystems, Dr. Antonio Cruzado (Ed.), ISBN: 978-
767 953-51-0176-5,InTech
768
769 Rey, A.R., Huettmann, F. (2020). Telecoupling analysis of the Patagonian Shelf: A new approach to
770 study global sea bird-fisheries interactions to achieve sustainability. Journal for Nature
771 Conservation, 53, 125748. https://doi.org/10.1016/j.jnc.2019.125748
772
773 Richard G., Vacquié-Garcia J., Jouma'a J., Picard B., Génin A., Arnould J.P.Y., et al. (2014).
774 Variation in body condition during the post-moult foraging trip of southern elephant seals and its
775 consequences on diving behaviour. J Exp Biol. 2014;217: 2609–2619. pmid:24803471
776
777 Richard G., Cox S.L., Picard B., Vacquié-Garcia J., Guinet C. (2016) Southern Elephant Seals
778 Replenish Their Lipid Reserves at Different Rates According to Foraging Habitat. PLoS ONE
779 11(11): e0166747. doi:10.1371/journal.pone.0166747
780
781 Rivas, A.L., Dogliotti A.I., Gagliardini D.A. (2006). Seasonal variability in satellite-measured
782 surface chlorophyll in the Patagonian Shelf; Pergamon-Elsevier Science Ltd; Continental Shelf
783 Research; 26; 6; 4-2006; 703-720
784

Romero S.I., Piola A.R., Charo M., and Garcia C.A. E. (2006). Chlorophyll-a variability off Patagonia based on SeaWiFS data. Journal of Geophysical Research, 111, C05021. https://doi.org/10.1029/2005JC003244

Roquet F., Charrassin J.-B., Marchand S., Boehme L., Fedak M., Reverdin G., and Guinet C. (2011). Validating hydrographic data obtained from seal-borne satellite-relayed data loggers. J. Atmosph. And Ocean. Tech., 28:787-801. doi: 10.1175/2010JTECHO801.1

Santini M.F., Souza R.B., Wainer I., Muelbert M.M. (2018). Temporal analysis of water masses and sea ice formation rate west of the Antarctic Peninsula in 2008 estimated from southern elephant seals' SRDL–CTD data. Deep Sea Research Part II: Topical Studies in Oceanography, Vol. 149, p58-69. https://doi.org/10.1016/j.dsr2.2018.02.013

Saraceno M., Provost C., Piola A.R., Bava J., & Gagliardini A. (2004). Brazil Malvinas Frontal System as seen from 9 years of advanced very high resolution radiometer data. *Journal of Geophysical Research C: Oceans*, *109*(5). https://doi.org/10.1029/2003JC002127

Saraceno M., Provost C., & Piola A.R. (2005). On the relationship between satellite-retrieved surface temperature fronts and chlorophyll a in the western South Atlantic. Journal of Geophysical Research: Oceans, 110(11), 1–16

Saraceno M., Provost C., & Zajaczkovski U. (2009). Long-term variation in the anticyclonic ocean circulation over the Zapiola Rise as observed by satellite altimetry: Evidence of possible collapses. Deep-Sea Research Part I: Oceanographic Research Papers, 56(7)

Schreer J.F., Kovacs K.M., O'Hara Hines R. J. (2001). Comparative diving patterns of pinnipeds and seabirds. Ecol Monogr. 2001;71: 137–162

Siegelman L., Roquet F., Mensah V., Rivière P., Pauthenet E., Picard B., and Guinet C. (2019). Correction and accuracy of high- and low-resolution CTD data from animal-borne instruments. Journal of Atmospheric and Oceanic Technology. doi: 10.1175/JTECH-D-18-0170.1

Stark J.D., Donlon C.J., Martin M.J. and McCulloch M. E. (2007). OSTIA: An operational, high resolution, real time, global sea surface temperature analysis system., Oceans 07 IEEE Aberdeen, conference proceedings. Marine challenges: coastline to deep sea. Aberdeen, Scotland. IEEE.

Violante R.A. and Cavallotto J.L. (2011). The record of the LGM sea-level position at the Argentina Continental Shelf: an evidence of the complex processes involved in the post-glacial relative sea level rise. In : Abstracts of the 5th IGCP 526 Conference 'Continental Shelves: Risks, Resources and Record of the Past', Victoria (BC), Canada. UNESCO-IGCP, Paris, 128–129

Violante R., et al. (2014). Chapter 6 The Argentine continental shelf: morphology, sediments, processes and evolution since the Last Glacial Maximum. 10.1144/M41.6.

Viviant M., Trites A.W., Rosen D.A. S., Monestiez P., Guinet C. (2010). Prey capture attempts can be detected in Steller sea lions and other marine predators using accelerometers. Polar Biol 33: 713–719